Hoxb1 Regulates Distinct Signaling Pathways in Neuromesodermal and Hindbrain Progenitors to Promote Cell Survival and Specification

Kristijan Pazur, Ioannis Giannios, Mathias Lesche, Eva Rodriguez-Aznar, Anthony Gavalas

Stem Cells, 2022, **40**, 175–189
https://doi.org/10.1093/stmcls/sxab014
Advance access publication 24 January 2022
Original Research

Hoxb1 Regulates Distinct Signaling Pathways in Neuromesodermal and Hindbrain Progenitors to Promote Cell Survival and Specification

Kristijan Pazur[1,2], Ioannis Giannios[1,3], Mathias Lesche[4], Eva Rodriguez-Aznar,[1,3,5] Anthony Gavalas[1,3,6,*]

[1]Paul Langerhans Institute Dresden (PLID) of Helmholtz Center Munich at the University Clinic Carl Gustav Carus of TU Dresden, Helmholtz Zentrum München, German Research Center for Environmental Health, Neuherberg, Germany
[2]Current address: Department of Dermatology and Allergy, Charité-Universitätsmedizin Berlin, Berlin, Germany
[3]German Centre for Diabetes Research (DZD), Düsseldorf, Germany
[4]Biotechnology Center (Biotec), TU Dresden, Dresden, Germany
[5]Current address: Oncology Research Center, Vrije Universiteit Brussel, Brussels, Belgium
[6]Faculty of Medicine, Center for Regenerative Therapies Dresden (CRTD), TU Dresden, Dresden, Germany

*Corresponding author: Anthony Gavalas, Fetscherstrasse 74, 01307 Dresden, Germany. Tel: 0049 (0) 351 7963 6630; Email: anthony.gavalas@tu-dresden.de

Abstract

Hox genes play key roles in the anterior-posterior (AP) specification of all 3 germ layers during different developmental stages. It is only partially understood how they function in widely different developmental contexts, particularly with regards to extracellular signaling, and to what extent their function can be harnessed to guide cell specification in vitro. Here, we addressed the role of *Hoxb1* in 2 distinct developmental contexts; in mouse embryonic stem cells (mES)-derived neuromesodermal progenitors (NMPs) and hindbrain neural progenitors.

We found that *Hoxb1* promotes NMP survival through the upregulation of *Fgf8*, *Fgf17*, and other components of Fgf signaling as well as the repression of components of the apoptotic pathway. Additionally, it upregulates other anterior *Hox* genes suggesting that it plays an active role in the early steps of AP specification. In neural progenitors, *Hoxb1* synergizes with shh to repress anterior and dorsal neural markers, promote the expression of ventral neural markers and direct the specification of facial branchiomotorneuron (FBM)-like progenitors. Hoxb1 and shh synergize in regulating the expression of diverse signals and signaling molecules, including the Ret tyrosine kinase receptor. Finally, Hoxb1 synergizes with exogenous Glial cell line-derived neurotrophic factor (GDNF) to strengthen Ret expression and further promote the generation of FBM-like progenitors. Facial branchiomotorneuron-like progenitors survived for at least 6 months and differentiated into postmitotic neurons after orthotopic transplantation near the facial nucleus of adult mice. These results suggested that the patterning activity of *Hox* genes in combination with downstream signaling molecules can be harnessed for the generation of defined neural populations and transplantations with implications for neurodegenerative diseases.

Key words: neuromesodermal progenitors; hindbrain; neural progenitors; Hox genes; embryonic stem cells; differentiation; Ret tyrosine kinase receptor; GDNF

Graphical Abstract

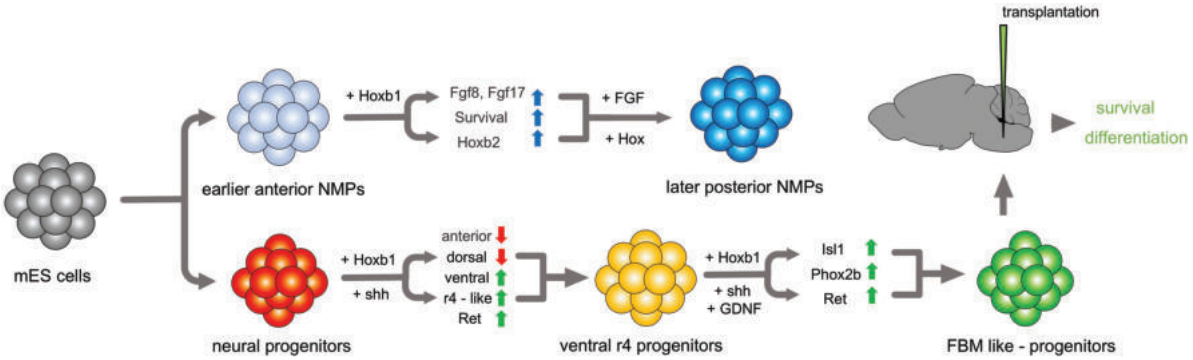

Received: 11 May 2021; Accepted: 28 October 2021.

Significance Statement

We have addressed the role of Hoxb1 in two distinct developmental contexts; in mouse embryonic stem cell-derived neuromesodermal progenitors (NMPs) and hindbrain neural progenitors. In both cellular contexts, *Hoxb1* regulates extracellular signaling promoting cell survival and further differentiation into appropriate cell times, raising the possibility that this is a widespread yet underappreciated aspect of *Hox* gene function. A multi-step approach combining the establishment of proper axial identity in human pluripotent stem cell-derived neuralmesodermal progenitors, and the subsequent timely application of appropriate signals could be the blueprint to generate motor neurons and neurons suitable for disease modeling and therapeutic approaches.

Introduction

Hox genes encode a highly conserved family of homeobox containing transcription factors that impart anterior-posterior (AP) information and thus are implicated in cell-type specification in a wide range of vertebrate tissues derived from all 3 germ layers. Loss and gain of *Hox* gene function can lead to homeotic transformations, meaning the change of a body part into the likeness of another. Whereas this has been a key hallmark of Hox protein function, there are numerous phenotypes in all 3 germ layers that do not conform to this simple framework. Different cellular functions are controlled by Hox proteins including changes in cell shape and migration, proliferation and programmed cell death as well as differentiation.[1,2] Functional compensation among *Hox* genes as well as their versatile and cell context-dependent activity have kept their functional modalities enigmatic, particularly regarding their diverse roles in tissues of all 3 germ layers. Additionally, their relaxed binding specificity can be only partially tightened through cooperative binding with the homeobox transcription factors of the Pbx and Meis families.[3] This is reflected in the generally large number of detected binding sites for some of the few vertebrate Hox proteins investigated.[4-10] It implies that interaction with additional transcription factors might be necessary to account for the context specific functions of *Hox* genes. Thus, despite the wealth of knowledge gained over decades of research on the molecular function of Hox genes, it is still only partially understood how they function in different developmental contexts, particularly with regards to extracellular signaling, and if their function can be harnessed to guide cell specification in vitro. Here, we have focused on *Hoxb1*, one of the earliest and most anteriorly expressed genes, and addressed its function in 2 distinct developmental contexts; neuromesodermal progenitors (NMPs), which give rise to both neural and mesodermal progenitors of the posterior vertebrate body, and hindbrain neural progenitors.

The early conceptual framework for the development of the nervous system postulated that the default state of the neural plate corresponded to anterior identity and that in a second step posterior identity was induced through the action of posteriorising signals such as Wnts and Fgfs.[11,12] The discovery of NMPs, bipotent cells that contribute to both the elongating spinal cord and paraxial mesoderm in the vertebrate embryo[13] provided compelling evidence that the posterior neural tissue develops through a distinct pathway. Fate mapping and transplantation studies established that NMP cells are located in the caudal lateral epiblast and adjacent to the node-streak border.[14,15] These bipotent progenitors are characterized by the simultaneous expression of the early mesodermal inducing transcription factor *Brachyury* (*Bra*) with the epiblast and neural transcription factor *Sox2*.[16] Inputs from both Wnt and FGF signaling are required in the induction and maintenance of NMPs.[9,16-18] Neuromesodermal progenitor cells that leave the CLE due to proliferation and axis elongation are exposed to higher levels of RA generated from the paraxial mesoderm and lower levels of FGF and Wnt signaling. This triggers their differentiation into either neural or mesodermal tissue. *Hox* genes are orderly activated during NMP expansion and NMP exit from this state fixes the Hox code acquired until then, thus establishing the AP axis of the posterior body.[19] A contribution of Hoxb1 to early induction of the neural crest territory has been postulated[20] but a potential role of *Hox* genes in NMPs has not been explored.

On the other hand, *Hoxb1* plays key roles in hindbrain patterning. The hindbrain coordinates sensory and motor functions of the head and autonomous functions essential for survival, including respiratory rhythm, motor activity, sleep and wakefulness. During development it is a transiently segmented structure organized into 8 lineage restricted compartments, the rhombomeres (r). Rhombomere restricted expression of anterior *Hox* genes and other transcription factors such as Krox-20 (expressed in r3, 5) and Kreisler (expressed in r5, 6) endows each segment with specific identity that guides their subsequent development to generate the appropriate neuronal populations, cranial nerves and neural crest derived structures.[21,22] *Hoxa1*, the paralog of *Hoxb1*, also partially in concert with Hoxb1 is necessary for proper hindbrain segmentation.[23-25] In order to generate neuronal subtype diversity within each AP segment, dorsoventral (DV) patterning signals have to be correctly interpreted and integrated into distinct differentiation programs. Dorsally, *Hoxb1* and *Hoxa1* synergize in patterning of the r4 and r4 derived neural crest derivatives of the pharyngeal arches. Either of them show small (*Hoxa1*) or no (*Hoxb1*) defects in neural crest specification when mutated individually but the combined mutation of *Hoxa1* and *Hoxb1* results in the loss of this cell population.[26,27] Ventrally, shh target *Nkx* genes cooperate with *Hoxb1* in r4 to maintain *Phox2b* expression and generate FBM neurons.[28] In *Hoxb1* mutant mice, initial segmentation and motor neuron generation occurs normally but the generated motor neurons are not specified correctly. They assume anterior, trigeminal identity, project axons inappropriately, fail to undergo their typical caudal migration to r4 and eventually die. As a consequence, the facial nucleus is lost in the *Hoxb1* null mice and the facial nerve is either lost or rudimentary.[29-31] Additionally, Hoxb1 participates in the formation of brainstem auditory nuclei during development.[32] Homozygous HOXB1 loss-of-function mutations in humans result in bilateral facial palsy and hearing loss, partly recapitulating the mouse phenotype.[33,34]

To bypass some of the limitations of in vivo studies regarding Hoxb1 function in different developmental contexts we used mouse ES cell directed differentiation as a model system. Mouse ES cells were differentiated into NMPs through the timely activation of Wnt and Fgf signaling[18]

or hindbrain neural progenitors using a neural selection medium and inducible *Hoxb1*[35] gene expression. We provide evidence that *Hoxb1* functions by regulating distinct signaling pathways and their readout to promote survival and specification.

Materials and Methods

Mouse Lines

Experiments and maintenance of animals was conducted in compliance with the FELASA recommendations and the ethical and practical guidelines for the care and use of laboratory animals set by the competent veterinary committees at the TU Dresden. The *Hoxb1*^{tm1Brd} (*Hoxb1*^{null}) mouse line used was generated by the in-frame insertion of a *lacZ* transgene in the first exon as well as the neomycin resistance cassette. Mice were genotyped using a standard PCR procedure. Primers used were: common forward primer for both wild type and *Hoxb1*^{null} (AGCTTCAGCTCTGTGACATACTGCCG), reverse primer for wild-type locus (CAGAATAATACTGAG AAGGCCCATAGCTGG) and reverse primer for *Hoxb1*^{null} recombinant locus (TAGATGGGCGCATCGTAACCGTGC).

Generation of Mouse ES Cell Lines

To generate mouse embryonic stem cells (mES) *Hoxb1*^{null} lines, heterozygous *Hoxb1*^{null} mice were timed mated and at 3.5 dpc the uterus was dissected and preimplantation blastocysts were flushed out. Blastocysts were cultured in gelatinized 96-well plate in 2i medium. 2i medium is comprised of 50% per volume of DMEM/F12 (Gibco, 21331-020) and Neurobasal medium (Gibco, 21103-049) supplemented with 0.8% BSA (Sigma, A8412), 0.5% N2 Plus Supplement (17502-048 Gibco), 0.5% B27 serum free Supplement (Gibco, 10889-038), 100 U/mL of penicillin/streptomycin (Life Technologies, 15140-122), 2 mM L-Glutamine (Life Technologies, 25030-081), 10^3 U/mL of LIF (Millipore, ESG1107), 1 μM PD03259010 (Stemgent, 130-0950557), and 3 μM CHIR99021 (Axon, 1386). Blastocysts were grown for 6 days with daily changing of medium. After initial expansion of blastocysts, surviving inner cell mass cells generated ES cells that were passaged every 2 days as described below.

Mouse ES cells allowing dox inducible expression of *Hoxb1* were further genetically modified using homologous recombination to constitutively express the fluorescent protein EGFP under the control of the strong CAG promoter. The EGFP sequence was amplified by PCR using a forward primer incorporating an AscI restriction site (underlined) (CACTAA *GGCGCGCC*ACCATGGTGAGCAA) and a reverse primer incorporating a SacI restriction site (GACTGCA*GAGCTC* TTACTTGTACAGCTCGTCC). The AscI/SacI digested PCR product was introduced in a similarly cut ROSA26 targeting vector containing the *5′* and *3′ Rosa26* homology arms, CAG promoter and a puromycin resistance cassette (gift from Konstantinos Anastassiadis). The targeting vector was linearized with SwaI, and ES cells were electroporated using the BTX electroporator (ECM630) and plated onto 100 mm TC-Treated Culture Dish (Corning, 207054). Cells were grown for 48 hours in normal mouse ES medium, and then were transferred to medium containing 1 μg/mL of puromycin for the selection of stable transformants. EGFP$^+$ clones were selected using live imaging with the EVOS Imaging System (Thermo Fisher, AMF4300). To detect clones with stable integration by homologous recombination into the *Rosa26* *L*ocus, Southern blot was used. Genomic DNA was extracted from cells by proteinase K digestion and isopropanol precipitation. DNA was digested with EcoRI overnight, separated on agarose gel and blotted to nylon membranes (Pall). Probes were made with ^{32}P by random priming (Roche Diagnostics) and hybridization was according to standard procedures.

Differentiation of Mouse ES Cells to NMPs and FBM Progenitor Cells

Mouse ES cells were grown on mouse embryonic feeder cells in Knockout Dulbecco's modified Eagle's medium medium (Life Technologies, 10829-018) supplemented with 10% stem cells grade fetal calf serum (PAN Biotech, 2902-P10171), 1× Non Essential Amino Acids (Life Technologies, 11140-035), 100 U/mL penicillin/streptomycin (Life Technologies, 15140-122), 2 mM L-glutamine (Life Technologies, 25030-081), and 10^3 U/mL of LIF (Millipore, ESG1107) and passaged at least 2 times before differentiation. Cells were detached using 0.05% trypsin-EDTA (Gibco, 25300-054) and feeder cells were panned out.

To differentiate mouse ES cells to NMP cells were plated at at a density of 5×10^3 cells/cm^2 on gelatinized Cell Bind dishes (Corning, CLS3294). The medium used was comprised of 50% per volume of DMEM/F12 (Gibco, 21331-020) and 50% Neurobasal medium (Gibco, 21103-049) supplemented with 0.8% BSA (Sigma, A8412), 0.5% N2 Plus Supplement (17502-048 Gibco), 0.5% B27 serum-free supplement (Gibco, 10889-038), 100 U/mL penicillin/streptomycin (Life Technologies, 15140-122), 2 mM L-glutamine (Life Technologies, 25030-081), and 10 ng/mL bFGF (Life Technologies, 13256-029). In order to generate NMPs, the medium was supplemented with 3 μM CHIR99021 (Axon, 1386) on the second day. Fgf8 (R&D 423-F8) or Fgf17 (R&D 7400-FG) was used (stage 2, Fig. 1D) at 25 ng/mL or 50 ng/mL, respectively. Cells were grown for 3 days with daily changes of medium.

For the differentiation to neuroepithelial cells, mouse ES cells were first seeded in mouse stem cell medium in bacterial plates (Sarstedt, 83.1801.002) at a concentration of 10^5 cells/mL in order to form EBs. EBs were grown for 4 days with changing of medium after 2 days. Then, EBs were plated in gelatinized 60mm TC-Treated Culture Dish (Corning, 430166) in ISTFn (Insulin-Selenium-Transferrin-Fibronectin) neural selection medium. The medium was comprised of DMEM/F12 (Gibco, 21331-020) supplemented with 100 U/mL penicillin/streptomycin (Life Technologies, 15140-122), 2 mM L-glutamine (Life Technologies, 25030-081), 5 μg/mL insulin (Sigma, I0516), 50 μg/mL transferrin (Gibco, 11107), 30 nM selenium, and 5 μg/mL fibronectin (Invitrogen, 33010-018). The selection stage lasted for up to 9 days and fresh medium was added every 2 days. After the selection stage, cell clusters were dissociated and the resulting neuroepithelial cells were expanded by plating them in 6-well plates (Corning, 3506) coated with Growth Factor reduced Matrigel Matrix (BD Biosciences, SPC-354230) at a concentration of 2×10^5 cells/cm^2, 2 mL cell suspension per well. Expansion medium was comprised of DMEM/F12 (Gibco, 21331-020) supplemented with 100 U/mL penicillin/streptomycin (Life Technologies, 15140-122), 2 mM L-glutamine (Life Technologies, 25030-081), 20 μg/mL Insulin (Sigma, I0516), 1% N2 Plus Supplement (17502-048 Gibco), 0.6% glucose (Sigma, G7021), and 10 ng/mL bFGF (Life Technologies, 13256-029). Cells were expanded for 4 days with fresh medium change

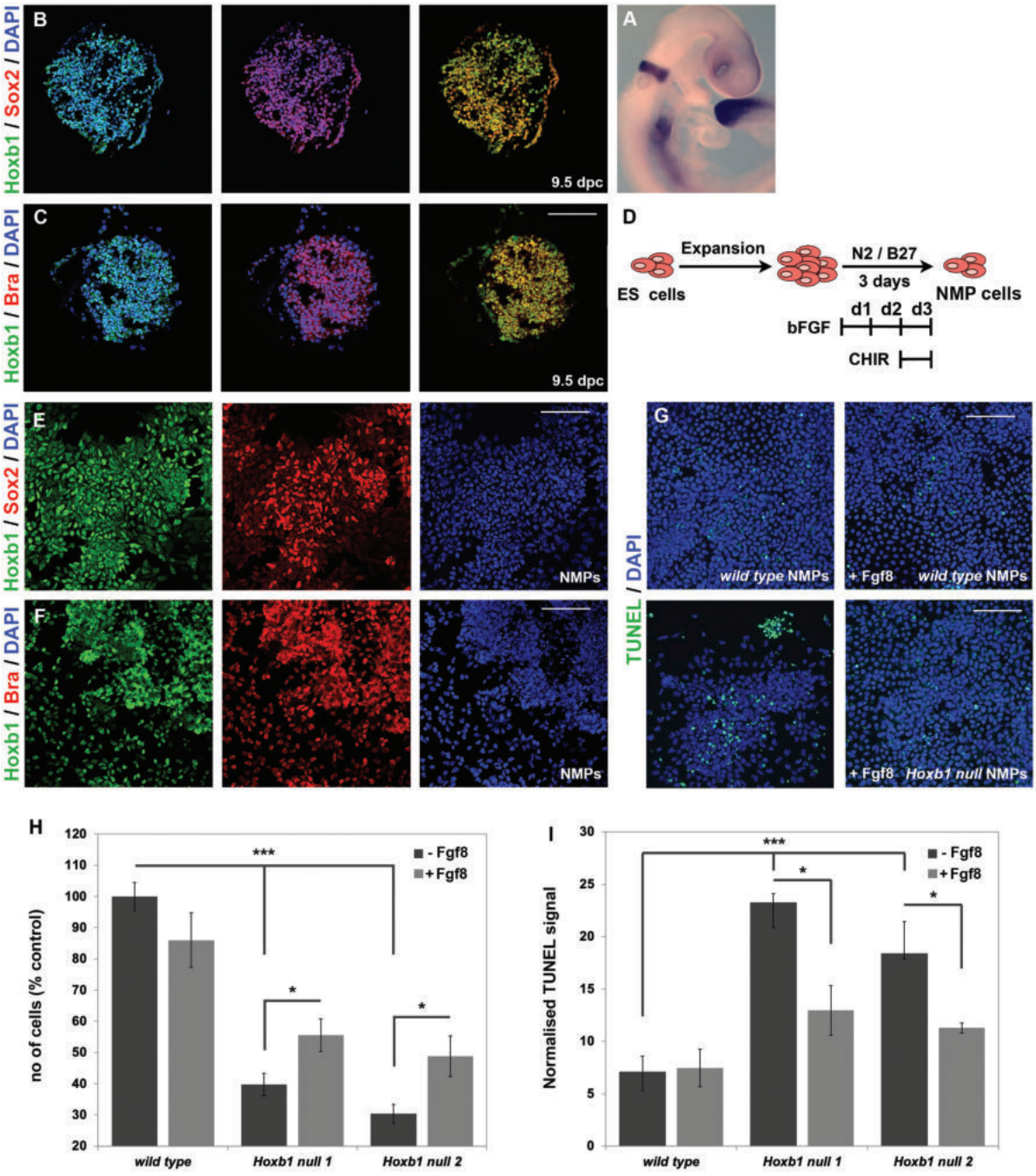

Figure 1. Hoxb1 is expressed in NMPs and promotes their survival.Sections through the NMP containing area of a 9.5-dpc developing embryo (A) and immunofluorescence revealed co-expression of Hoxb1 with the NMP markers Sox2 (B) and Bra (C). In mES-derived NMPs as shown (D) Hoxb1 is co-expressed with Sox2 (E) and Bra (F). There is excessive cell death as assayed by TUNEL in *Hoxb1 null* NMPs (G, I) (n = 3) resulting in lower number of cells (H) (n = 4-7). Cell death is reduced by the addition of Fgf8 (G, I) (n = 4-5) and this leads in partial restoration of cell numbers (H). These effects were assessed in 2 independently derived *Hoxb1 null* mES lines (*null 1, 2*). Scale bars correspond to 100 µm; * $P < .05$ and *** $P < .005$; error bars show ± SEM.

every second day. In order to induce expression of *Hoxb1* and activate the r4-specific genetic program doxycycline (Sigma, D9891) was used at a concentration of 1 µg/mL during the selection and expansion stages. Ventralization of the neuroepithelial cells was achieved by treating the cells with 200 nM of shh agonist SAG (ALEXIS, ALX-270-426-M001) during the expansion stage. For further differentiation, cells were passaged once and grown in 6-well plates on Growth Factor reduced Matrigel Matrix in expansion medium in which bFGF was substituted with 50 ng/mL GDNF (Sigma, SRP3200).

RNA Isolation and Real-Time PCR

Total RNA was prepared using the RNeasy kit with on-column genomic DNA digestion following the manufacturer's instructions (Qiagen). First-strand cDNA was prepared using Superscript II RT (Invitrogen). Real-time PCR primers were designed using the Primer 3 software (SimGene) and specificity was ensured by In Silico PCR. Reactions were performed with SYBR-GreenER (Invitrogen) using a Roche LC480 machine and primary results were analyzed using the on board software. Reactions were carried out in

duplicate from at least 3 independent samples. Absolute expression values were calculated using the ΔCt method and *β-actin* was used for normalization. Primers used were further evaluated by inspection of the dissociation curve. Primer sequences were as follows: Ret-Fw: GCAGGAGCCA GACAAGAGG, Ret-Rev ATACAGCAGTGAGTCCGAA GG β-actin-Fw: TGGCTCCTAGCACCATGA, β-actin-Rv: CCACCGATCCACACAGAG.

Immunofluorescence and TUNEL Analysis

Differentiated cells in culture were fixed in 4% paraformaldehyde (PFA) for 15 minutes at 4 °C. Mouse embryos were dissected at the appropriate stage and fixed in 4% PFA at 4 °C for 1 hour, cryoprotected in 20% sucrose solution, embedded in optimal cutting temperature compound and cryosectioned to 10 µm thick sections. Regarding mouse adult brains, animals were first perfused with 20 mL of 4% PFA under general anesthesia. Mouse brains were then dissected, post fixed in 4% PFA overnight at 4 °C and embedded in 4% low melting agarose in PBS. Brains were then vibratome sectioned into 50 µm thick sections. All specimens were then processed for immunofluorescence using standard procedures. Specifically for the goat anti-Ret antibody the signal was amplified using the TSA Plus Fluorescent system kit (Perkin Elmer, NEL753). Cell death was detected using In Situ Cell Death Detection Kit (Roche, 11684795910) according to manufacturer's instruction.

Primary antibodies used were: rabbit anti-PH3 (1:500, Cell signaling), rabbit anti-Hoxb1 (1:200, Covance), mouse anti-Nkx2.2 (1:50, Jessell T.M), mouse anti-Pax6 (1:50, DSHB, Atsushi Kawakami), mouse anti-Pax7 (1:10, DSHB, Atsushi Kawakami), mouse anti-Islet1 (1:100, DSHB, Tom Jessell), mouse anti- β-tubulin class III (1:1000, Covance), mouse anti-Neu N (1:500, Chemicon), rabbit anti-Pax6 (1:1000, Chemicon), mouse anti-Nkx6.1 (1:1000, DSHB, Madsen), rabbit anti-Sox2 (1:500, Millipore, AB5603), goat anti-Sox2 (1:40, R&D Systems, AF2018), goat anti- Brachyury (1:500, R&D Systems, AF2085), rabbit anti-Phox2b (1:200, a gift from J.F.Brunet), goat anti-Ret (1:20, Santa Cruz, sc-167-G), rabbit anti-Tbx20 (1:200, Santa Cruz, sc-134061), mouse anti-GFP (1:1000, Abcam, ab1218), goat anti-ChAT (1:100, Merck, AB144P), and mouse anti-FLAG M2 (1:1000, Sigma, F1804). Secondary antibodies used were: goat anti-rabbit Alexa fluor 488 (1:500, Molecular probes), goat anti-mouse Alexa fluor 568 (1:500, Molecular probes), goat anti-rabbit Alexa fluor 568 (1:500, Molecular probes), goat anti-mouse Alexa fluor 488 (1:500, Molecular probes), donkey anti-goat Alexa fluor 568 (1:500, Molecular probes), and donkey anti-goat peroxidase (1:750, Jackson). All samples were imaged using the upright laser scanning confocal microscope Leica TCS SP5.

Morphometric and Statistical Analyses

All morphometric analyses were performed using immunofluorescent images taken at saturation and the ImageJ software. Control and experimental samples were photographed and processed using identical conditions. The "Find maxima" tool of Fiji was used to quantitate total TUNEL and PH3 signal that mark cell death and proliferation. The signal was smoothened using the Gaussian Blur filter to reduce image noise due to the fragmented signal of the TUNEL and PH3 stainings. Signal was normalized for the total number of cells which was estimated by measuring the total DAPI area that corresponds to all nuclei. Cell death and proliferation was calculated as a ratio of the TUNEL or PH3 signal over total DAPI signal. Quantitation of immunofluorescence signal for nuclear markers in differentiated cells was calculated by counting all cells with positive nuclear signal and divided by the total number of cells. The overlap between Phox2b and Isl1 staining was estimated using the Coloc 2 function of Fiji.

Statistical significance was determined by the Student's *t* test for 2-tailed distributions of unpaired groups. The SEM is provided and $P < .05$ was considered significant.

RNA Sequencing and Bioinformatics Analyses

Neuroepithelial and NMPs were differentiated from mouse ES cells as described above. Three independent samples from distinct differentiations were used as biological replicates. Total RNA prepared as above with an integrity number of ≥9 was used and subsequent steps were performed at the Biotec Sequencing Core of TU Dresden. mRNA was isolated from 1 µg of total RNA by poly-dT enrichment using the NEBNext Poly(A) mRNA Magnetic Isolation Module according to the manufacturer's instructions. Final elution was done in 15 µL 2× first strand cDNA synthesis buffer (NEBnext, NEB). After chemical fragmentation by incubating for 15 minutes at 94 °C the sample was directly subjected to the workflow for strand specific RNA-Seq library preparation (Ultra Directional RNA Library Prep, NEB). For ligation custom adaptors were used 1: (Adaptor-Oligo 5′-ACA CTC TTT CCC TAC ACG ACG CTC TTC CGA TCT-3′, Adaptor-Oligo 2: 5′-P-GAT CGG AAG AGC ACA CGT CTG AAC TCC AGT CAC-3′). After ligaton adapters were depleted by an XP bead purification (Beckman Coulter) adding bead in a ratio of 1:1. Indexing was done during the following PCR enrichment (15 cycles) using custom amplification primers carring the index sequence indicated with "NNNNNN". (Primer1: Oligo_Seq AAT GAT ACG GCG ACC ACC GAG ATC TAC ACT CTT TCC CTA CAC GAC GCT CTT CCG ATC T, primer2: GTG ACT GGA GTT CAG ACG TGT GCT CTT CCG ATC T, primer3: CAA GCA GAA GAC GGC ATA CGA GAT NNNNNN GTG ACT GGA GTT. After 2 more XP beads purifications (1:1) libraries were quantified using Qubit dsDNA HS Assay Kit (Invitrogen). For Illumina flowcell production, samples were equimolarly pooled and distributed on all lanes used for 75bp single read sequencing on Illumina HiSeq 2500.

After sequencing, FastQC (http://www.bioinformatics.babraham.ac.uk/) was used to perform a basic quality control on the resulting reads. As an additional control, library diversity was assessed by redundancy investigation in the mapped reads. Alignment of the short reads to the mm9 transcriptome was performed with gsnap (2014-12-17)[36,37] and a table of read counts per gene was created based on the overlap of the uniquely mapped reads with the Ensembl Genes annotation v. 69 for mm10, using Feature Counts (v1.4.6).[38] Normalization of the raw read counts based on the library size and testing for differential expression between the different cell types/treatments was performed with the DESeq R package (v. 1.8.1).[39] Sample-to-sample Euclidean distance as well as Pearson's correlation coefficient (*r*) were computed based on the normalized gene expression level in order to explore correlation between biological replicates and different libraries. For testing for differential expression, the count data were fitted to the negative binomial distribution and the *P*-values for the statistical significance of the fold change were adjusted for multiple testing with the Benjamini-Hochberg correction

for controlling the false discovery rate. Accepting a maximum of 10% false discovery rate (FDR) (padj ≤ 0.1), genes with normalized counts > 100 in either null samples or controls and fold change < 0.6 or >1.6 were considered as regulated. Heat maps for regulated genes with normalized counts ≥100 in at least one time point and condition were generated by calculating the *z* score for each condition in each sample (*z* score = (normalized gene counts – mean of normalized counts)/(standard deviation/√number of samples)). Heatmaps were generated with the R package pheatmap (1.0.8). We used the values from the rlogTransformation function of DESeq2 for the calculation of the *Z*-score. Original RNA Seq data have been deposited in GEO under the GSE174021 accession number and accessible with the token adyxkscclhypber.[40] GO and KEGG analyses have been carried out using the DAVID suite (https://david.ncifcrf.gov/home.jsp).[41,42]

Transplantation of Neural Progenitors in the Bra in

To generate the glass needs for the cell transplantations, glass capillaries (Harvard Apparatus, borosilicate glass GC120TF-10, 30-0050) were placed into the capillary puller machine (Sutter instruments, P-97) equipped with a closed platinum 350 filament. Long (approximately 1 cm) but thin capillaries with an outer diameter 90-95µm and inner diameter 70-80 µm were generated using the following conditions: pressure = 500, heat = 895, pull = 35, velocity = 35, time = 50. One day before using, capillaries were coated with Sigmacote (SL2-25ML) and sterilized under UV light.

Eight-week-old C57/Bl6 mice were placed in the anesthesia box under isoflurane anesthesia (2% isoflurane in O_2). Once deep anesthesia was achieved, the animal was transferred to the stereotactic frame on an electrically heated pad. The head was fixed on the stereotactic device using ear bars and the teeth holder with continuous delivery of oxygen and isoflurane through a mouth mask. Antiseptic eye cream was applied on the eyes for corneal protection. The head was shaved and 10% antiseptic betadine solution was applied. The operation started by making an incision along the sagittal suture line. The skull was dried with a cotton swap and the skin was pulled out of the surgical field. The initial setting of injector was placed to the coordinate (0, 0) after pointing the glass capillary needle (dimensions OD = 90-95 µm, ID = 70-80 µm) at the Bregma. Holes of 1 mm diameter were drilled at the selected coordinates (anterior-posterior, AP; medio-lateral, ML): AP –5.85 mm, ML ±1.25 mm, using an ultrafast drill equipped with an automatic stop system to prevent damage to the brain tissue (David Kopf Instruments Model 1474). The moisture of the exposed skull and brain was maintained using PBS solution every few minutes. The glass capillary needle filled with 2.5 µL of the cell suspension was moved to desired coordinates and using the vertical knob the needle was moved until it gently touched the brain surface. This was set as DV coordinate 0. The needle was then set at the desired position and the capillary was introduced into the brain parenchyma at selected depth of –5,75 mm. The cell suspension was injected slowly as a total volume of 1000 nL at a rate of ~3 nL/s. The injected solution was left to diffuse into the brain parenchyma for 5 minutes after injection and then the capillary was withdrawn slowly at rate of ~1 mm/minute. The skin was placed back in position and sutured using 5-0 Coated VICRYL Plus Antibacterial thread. The wound was sterilized with Betadine and the mouse was transferred to a pre-warmed cage for recovery. Post-operative rehydration and analgesia were provided by injecting 1 mL of sterile 0.9% NaCl solution and 0.1 ml of carprofen (dosage of 5 mg/kg) subcutaneously. After transplantation animals were monitored daily. Six months after transplantation, the experimental mice were sacrificed and the brains were collected and further analyzed.

Results

Hoxb1 Promotes Survival in NMP Cells by Enhancing Fgf Signaling

Neuromesodermal progenitor cells are located in the node-streak border and in the adjacent caudal lateral epiblast of the developing embryo and are defined by the simultaneous expression of Sox2 and Bra.[16] Whole mount in situ hybridization at 8.5 and 9.5 dpc suggested the possibility that *Hoxb1* is expressed in NMP cells[43] and co-immunofluorescence experiments confirmed this hypothesis (Fig. 1A-C) raising the question of the functional significance of Hoxb1 expression in NMPs. *Hoxb1* null embryos do not show defects in the elongation of the posterior part of the body.[30,31] Consistent with that, TUNEL and PH3 immunofluorescence experiments did not suggest aberrant cell death or decreased proliferation in *Hoxb1*^{tm1Brd} null (*Hoxb1* null) embryos (Supplementary Fig. S1A, B).

To investigate the possible role of Hoxb1 in NMPs and to bypass possible compensatory mechanisms from surrounding tissues or strong expression of other Hox genes in this population in vivo, we generated isogenic wild type and *Hoxb1* null ES cells in 2i medium[44] from blastocysts originating from the intercross of *Hoxb1* heterozygotes. Consistent with the in vivo findings, ES derived NMPs (Fig. 1D) co-express Sox2, Bra, and Hoxb1 (Fig. 1E, F, Supplementary Fig. S1C). However, 2 independently derived clones of *Hoxb1* null ES cells (*Hoxb1* null 1, 2) consistently generated fewer NMP cells (Fig. 1I). This was due to excessive cell death, as assessed by TUNEL assays (Fig. 1G, J), but not in a change to proliferation rates, as assessed by PH3 immunofluorescence (S1F-H), suggesting that *Hoxb1* expression contributes specifically to NMP survival.

To identify potential Hoxb1 downstream effectors in NMP cell survival, we derived and compared the RNA Seq expression profiles of wild type and *Hoxb1 null* NMPs. Gene Ontology (GO) and KEGG analysis suggested affected pathways including AP patterning, apoptosis, and the MAPK signaling pathway (Supplementary Fig. S1D). Several *Hox* genes, primarily anterior ones, were downregulated in the *Hoxb1* null NMP cells consistent with the hypothesis that Hoxb1 is an important player in initiating posterior patterning at the NMP stage (Supplementary Table S1). Importantly, a large number of genes implicated in the apoptotic process were also regulated by Hoxb1 (Supplementary Table S1). Moreover, Fgf8 and Fgf17 as well as the positive regulator of Fgf signaling, Fgfbp1, were downregulated in *Hoxb1* null NMPs (Supplementary Table S2). Fgf signaling plays key roles in maintaining the stem cell zone and in NMP lineage allocation[45] and Fgf8 as well as Fgf17 are strongly expressed in the posterior part of the developing embryo.[46] Fgf8 and Fgf17 belong to the same subfamily and bind preferentially to the Fgfr1 that is the only FGF receptor strongly expressed in NMPs (Supplementary Table S3). On the other hand, NMPs derived from either wt or *Hoxb1* null mES cells were very

similar in their expression profile regarding the core markers of NMP identity[47] (Supplementary Fig. S1D and Table S1), suggesting that Hoxb1 does not contribute substantially in NMP specification per se.

To establish a role of Hoxb1 in *Fgf* regulation and NMP survival, we examined whether addition of Fgf8 to the medium during differentiation could rescue the cell death phenotype. Indeed, addition of 25 ng/mL of Fgf8 in the culture medium at the start of the second day until the end of the differentiation partially rescued cell numbers. TUNEL and proliferation assays showed that the increase in cell numbers was due exclusively to increased cell survival (Fig. 1G-J, Supplementary Fig. S1F-H). Surprisingly, Fgf17 did not have a similar effect even at 50 ng/mL (Supplementary Fig. S1I) suggesting a differential ability of these Fgfs to mediate NMP survival under these culture conditions.

Taken together, the data suggested that Hoxb1 does not participate in NMP specification but promotes NMP survival through the regulation of Fgf signaling and the apoptotic pathway. Additionally, Hoxb1 upregulates the expression of some, primarily anterior, *Hox* genes, suggesting that it plays an active role in the initiation of the posterior program in NMPs.

Hoxb1 and shh Signaling Synergize in Inducing FBM-Like Progenitors In Vitro

We then aimed to examine the role of Hoxb1 in the specification of FBM neural progenitors in concert with extracellular signals, shh in particular. Hoxb1 is essential for the segmental identity of FBM progenitors as well as the survival of FBMs themselves but details of its function at the molecular level remain elusive.[29-31] It has also been shown that doxycyclin (dox) inducible Hoxb1 expression in mES (ES $^{\text{Tet-On Hoxb1}}$)-derived neural progenitors results in a mixture of DV neural progenitors with hindbrain r4-like identity through the repression of anterior neural fates.[35] Here we reexamined these effects as well as the combined effects of Hoxb1 expression and stimulation of shh signaling. The number of Hoxb1$^+$ cells was negligible in the absence of dox and similar in dox or dox/ shh agonist (SAG) treated cells[48] (Supplementary Fig. S2A). Of note, and similar to the findings in the NMP state, Hoxb1 expression did not affect proliferation rates of progenitors under the culture conditions used (Fig. 2B).

RNA Seq (Fig. 2A) analysis followed by GO and KEGG analyses suggested that *Hoxb1* and shh signaling synergized in modulating a large number of process and molecular functions in neural progenitors (Supplementary Fig. S2C-E). Close analysis showed that induction of *Hoxb1* represses expression of anterior markers in neural progenitors (Supplementary Fig. S2F) and enriches dorsal identities as assessed by immunofluorescence (compare Fig. 2B-E with Fig. 2J-M, and see quantifications in Fig. 2R-U) and gene expression (Fig. 2V, Supplementary Fig. S2F and Table S4). This is consistent with the finding that Hoxb1 can promote the formation of neural crest in vivo.[20]

Facial branchiomotorneuron progenitor markers were not significantly upregulated in Hoxb1$^+$ cells (Fig. 2W). As expected, stimulation of shh signaling alone, repressed dorsal markers such as Pax6 and Pax7 and upregulated ventral markers such as Nkx6.1 and Nkx2.2 in mES-derived neural progenitors in both the protein (compare Fig. 2B-E with F-I, see quantifications in R-U) as well as transcript levels (Fig. 2V, Supplementary Table S4). It is interesting to note that, in anterior cells, upregulation of Nkx2.2 upon shh stimulation was robust whereas there was no Nkx6.1 upregulation reflecting the extensive expression of Nkx2.2 in the forebrain and the corresponding lack of Nkx6.1 there.[49,50]

We then asked whether Hoxb1 (+ dox) and shh (+ SAG) may synergize in regulating the expression of ventral markers in general and markers of FBM progenitors[51] in particular. Indeed, their combination further repressed dorsal markers and promoted cell differentiation towards a ventral phenotype as assessed by the expression of dorsal and ventral markers at the protein (compare Fig. 2B-M with N-Q and see quantifications in R-U) and transcript (Fig. 2V, Supplementary Table S4) levels. We have not directly compared immunofluorescence markers in the + shh and + dox groups as this would compare the effect of shh signaling on anterior cells to that of Hoxb1 expression in anterior cells.

Remarkably, the combined Hoxb1 expression and Shh mediated ventralization resulted in the dramatic shift to an r4-MNP like (FBM) identity with the coordinated upregulation, at the transcript level, of several FBM progenitor markers that were weakly expressed in the presence of dox or shh alone. A small number of these markers were downregulated, suggesting that additional signals might be necessary for complete specification (Fig. 2W, Supplementary Table S4). Furthermore, combination of Hoxb1 expression and shh signaling further sharpened AP cellular identity by repressing the expression of anterior hindbrain genes (*Pax2*, *Gbx2*, and *En1*) as well as *Mafb* (aka *Kreisler*) which is a marker of r5 (Supplementary Fig. S2F).

Thus, Hoxb1 and shh signaling act synergistically in further sharpening hindbrain identity, repressing dorsal neural markers and induce the specification of FBM-like progenitors in ES derived neural cells.

Shh and Hoxb1 Synergize in Regulating the Expression of Signals and Signal Receptors

The identification of specific signals and signal receptors for MN progenitor subpopulations will help refine specification and maturation of distinct motor neuron subclasses from pluripotent stem cells. The analysis of the RNA Seq data of our in vitro generated of FBM-like progenitors identified a large number of signals and signal receptors coordinately regulated through the synergistic action of Hoxb1 and shh (Fig. 3A, Supplementary Fig. S3A, B). These included the Ret receptor tyrosine kinase that mediates MN survival and has been identified as a downstream target of Hox proteins in motor neurons of the trunk.[52] These results suggested that Ret expression is downstream of Hoxb1 in FBM progenitors as well, and to assess this we first analyzed Ret expression in wild type and *Hoxb1^{null}* embryos.

Expression of Ret receptor in the developing Hoxb1$^+$ FBMs was first detected at 11.5 dpc in both r4 and r5 (Fig. 3B-D, Supplementary Fig. S4A-C). At this stage caudally migrating FBMs are Isl1$^+$, Tbx20$^+$ and Phox2b$^+$ and can be detected in both r4 and r5 (Fig. 3E-H, Supplementary Fig. S4D-G).[29,51] In *Hoxb1* null embryos, Isl1$^+$ MN progenitors are still born in r4 but do not express Tbx20 or Phox2b and migrate ectopically in a pattern similar to that of Hoxa2$^+$ trigeminal MNs[29-31,51] (Fig 3I). Loss of orthotopic Ret expression in the *Hoxb1* null embryos was consistent with the loss of FBM progenitors; however, expression was retained in the area of ectopically migrating MNs, suggesting that additional Hox proteins,

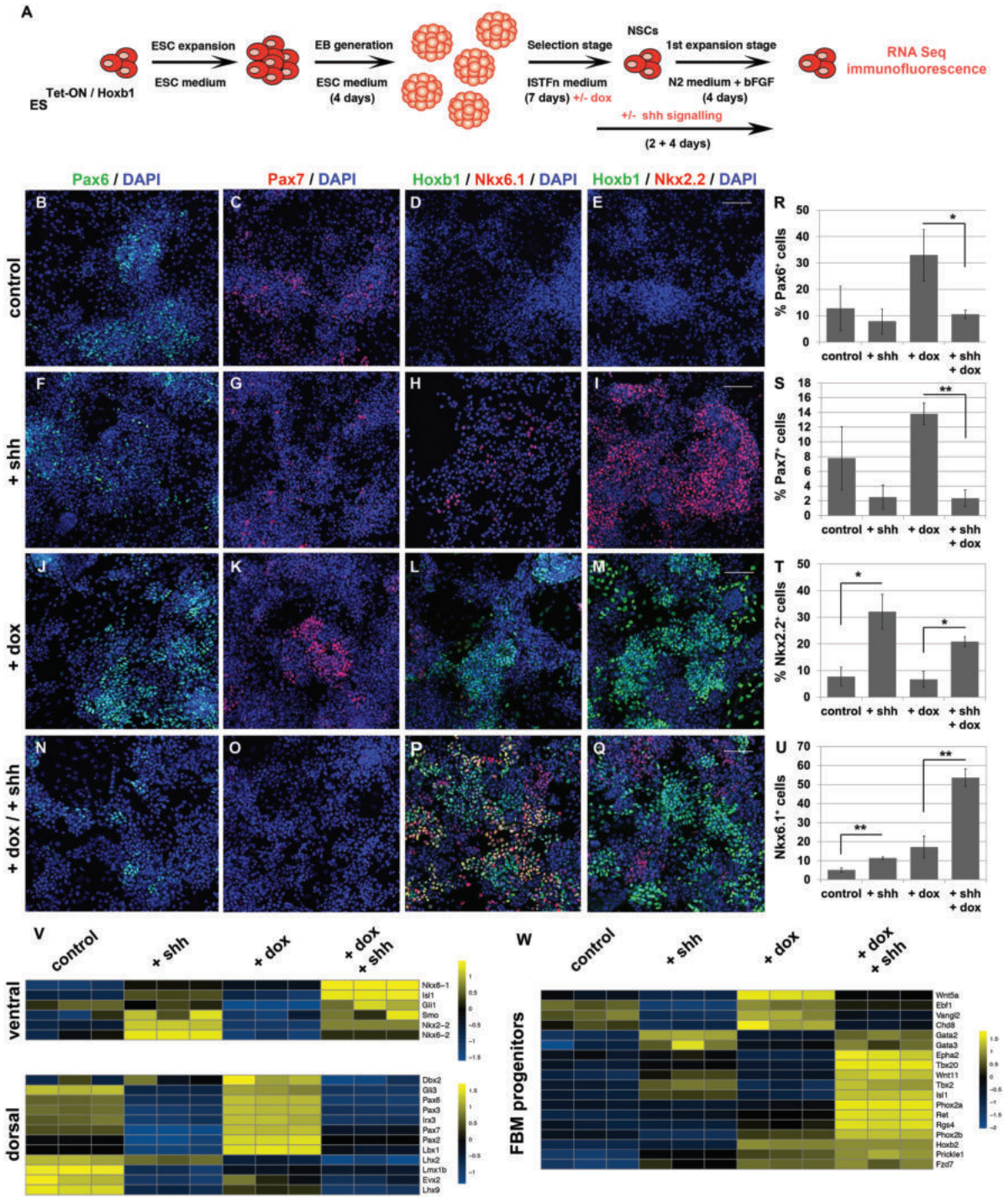

Figure 2. Hoxb1 and shh synergize in the specification of FBM progenitors. (**A**) The differentiation scheme leading from mES cells to neural progenitors. Experimental parameters and analyses are shown in red (**B**-**Q**) Immunofluorescences analysis of the expression of Pax6 (B, F, J, N), Pax7 (C, G, K, O), Hoxb1 (D, H, L, P, E, I, M, Q), Nkx6.1 (D, H, L, P), and Nkx2.2 (E, I, M, Q) in control cells (B-E), after stimulation of shh signaling (F-I), following Hoxb1 induction (J-M) or under combined Hoxb1 induction and shh stimulation (N-Q). Quantification of the number of Pax6$^+$ cells (R), Pax7$^+$ cells (S), Nkx2.2$^+$ cells (T) and Nkx6.1$^+$ cells (U) in different culture conditions ($n = 3$). Heat maps depicting changes of expression (z-score) under different conditions of DV markers (V) and FBM progenitor markers (W). Scale bars correspond to 200 µm; * $P < .05$ and ** $P < .01$; error bars show ± SEM.

primarily Hoxa2, maintain expression of Ret (Fig. 3I-L, Supplementary Fig. S4H-K).

Activation of Ret signaling through the addition of GDNF in organotypic hindbrain cultures resulted in an increase of *Ret* expression in FBMs.[53] To assess to what extent ES-derived FBM progenitors resemble their in vivo counterparts and whether Hoxb1 plays a role in *Ret* induction, mES-derived neural progenitor cells were exposed to 50 ng/mL GDNF during the expansion stage of differentiation (Fig. 2A) and levels of *Ret* expression were assessed by RT-qPCR. *Ret* expression was relatively low in control neural progenitors and this did not change upon shh stimulation, GDNF stimulation or a combination of both. In contrast, Hoxb1 synergized with shh signaling to induce *Ret* expression by nearly 3-fold

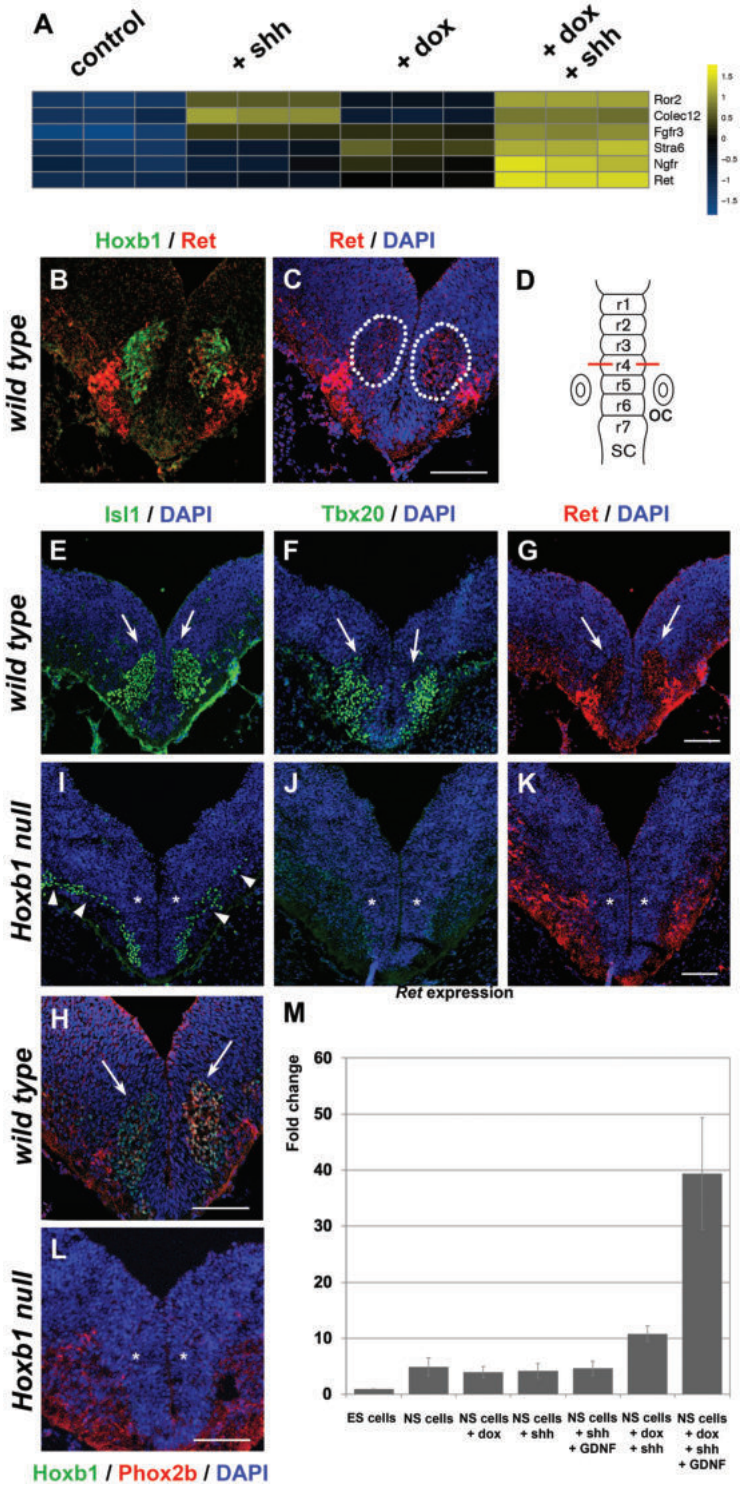

Figure 3. Ret expression is downstream of Hoxb1 in FBM progenitors in r4. (**A**) Heat map of the expression (*z*-score) of selected signal receptors demonstrating that Hoxb1 and shh synergize in the regulation of their expression in mES-derived FBM progenitor cells. Transverse sections at the level of r4 (**D**) of 11.5 dpc mouse embryos and immunofluorescence analysis shows that Ret is expressed in Hoxb1^{+} FBM progenitors in r4 (**B**, **C**). Immunofluorescence analysis for Isl1 (**E**, **I**), Tbx20 (**F**, **J**), Ret (**G**, **K**) and Phox2b with Hoxb1 (**H**, **L**) in wt (E, F, G, H) and *Hoxb1* null (I, J, K, L) embryos shows the loss of FBM progenitors and corresponding Ret expression in the *Hoxb1* null embryos. (**M**) Ret expression in FBM progenitors derived from mES cells is potentiated by Hoxb1 and its ligand, GDNF ($n = 3$ for NS + shh and NS cells + shh + GDNF, for all others $n = 6$). Arrows show the presence of FBM progenitors and stars their absence, whereas arrowheads ectopically migrating misspecified FBM progenitors. Scale bars correspond to 100 μm; * $P < .05$; error bars show ± SEM.

over levels in control neural progenitors. Further stimulation with GDNF stimulated *Ret* expression in Hoxb1 expressing cells by an additional nearly 3-fold, suggesting that Hoxb1 mediates the GDNF effect on *Ret* expression (Fig. 3M). The Hoxb1-mediated *Ret* upregulation was consistent with the ex vivo findings in embryonic FBMs further confirming that the

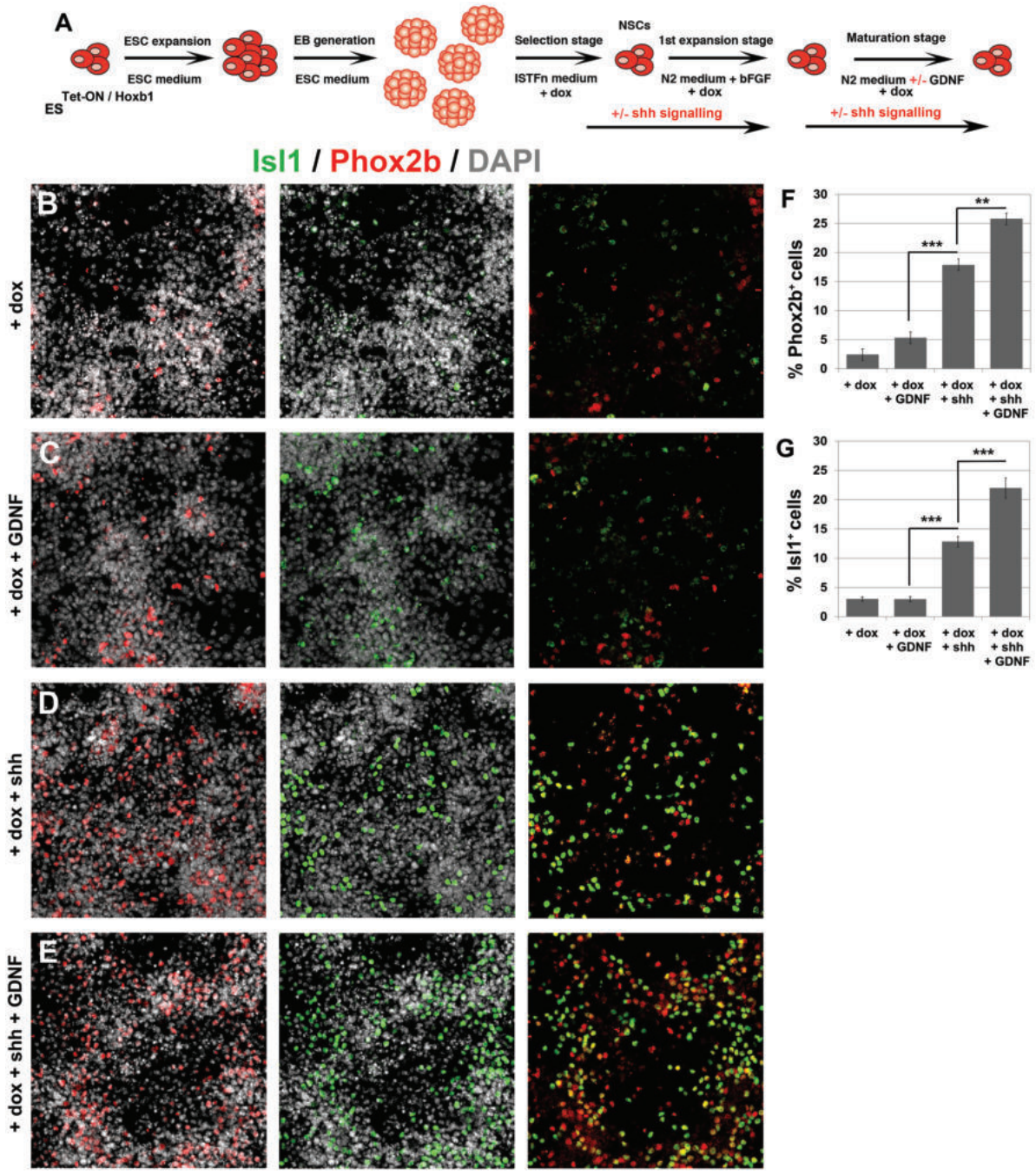

Figure 4. GDNF promotes the appearance of Phox2b⁺ and Isl1⁺ cells in mES-derived FBM-like progenitors. (**A**) The differentiation scheme for the generation of FBM progenitors and maturation in the presence of GDNF. Experimental parameters are shown in red. (**B**, **C**) Immunofluorescence analysis of FBM progenitors in the presence of dox (B), dox and GDNF (C), dox and shh signaling (**D**) or all 3 (**E**) for Phox2b and Isl1 expression and quantification (**F**, **G**) ($n = 4$) suggested that Hoxb1 synergizes with both shh signaling and GDNF in the induction of Phox2b⁺ and Isl1⁺ FBM-like progenitors. Scale bars correspond to 100 μm; ** $P < .01$, *** $P < .001$; error bars show ± SEM.

mES-generated FBM progenitors were quite similar to their in vivo counterparts.

This result raised the possibility that GDNF may promote the appearance of FBM-like progenitors in Hoxb1⁺ mES-derived neural cells exposed to shh signaling. To address this, we extended the culture of FBM-like progenitors for 4 additional days in the presence of 50 ng/mL GDNF (Fig. 4A) and assessed the appearance of Isl1⁺ and Phox2b⁺ cells by immunofluorescence (Fig. 4B-G). Whereas the number of Isl1⁺ and Phox2b⁺ cells was negligible in the presence of GDNF (≤5%), shh signaling resulted in the appearance of numerous Isl1⁺ and Phox2b⁺ cells. Combination of shh signaling and GDNF further increased the number of both Isl1⁺ and Phox2b⁺ cells (Fig. 4B-G). Image co-localization analysis suggested that, while inclusion of GDNF did not increase the estimated 86 ± 2% of Phox2b⁺ cells that were also Isl1⁺, it significantly increased the estimated 49 ± 2% of Isl1⁺ cells that were also Phox2b⁺ to 68 ± 4% ($P < .05$).

Taken together these results suggested that Hoxb1 and shh synergize in regulating the expression of a large number

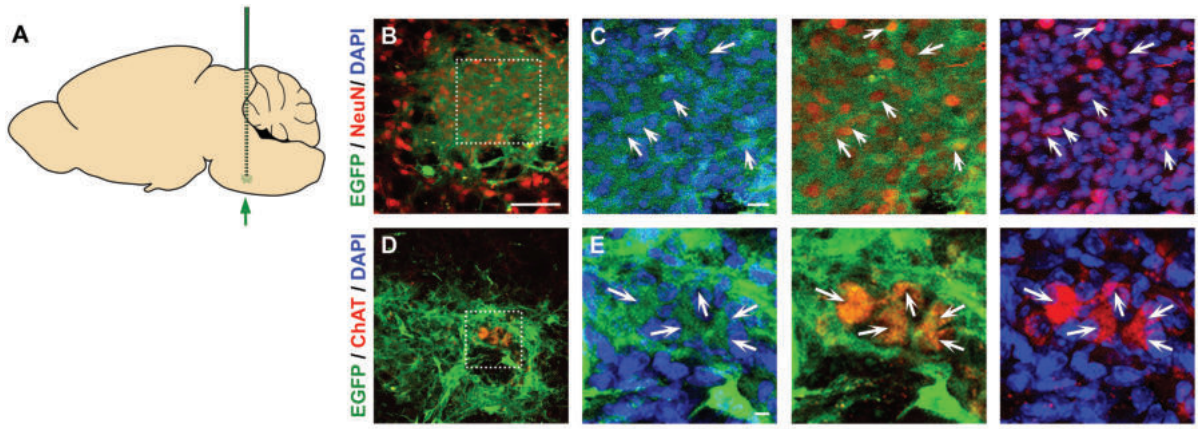

Figure 5. FBM-like progenitors survive well and become post-mitotic following ortotopic transplantation. (**A**, **B**, **D**) orthotopically transplanted FBM-like neural cells survive at least 6 months after transplantation, become post-mitotic NeuN⁺ cells (B) and occasionally express ChAT (D). (**C**, **E**) High magnification of the marked areas in (B) and (D) respectively show colocalization of EGFP and NeuN in the same cells (arrows in C mark some double-positive cells) as well as of EGFP (arrows in E mark the double-positive cells) and ChAT, respectively. Scale bars correspond to 50 μm.

of extracellular signals and signal receptors. Together, they strongly upregulate expression of the Ret tyrosine kinase receptor and this, in combination with the Ret ligand GDNF, may trigger a feed-forward loop to strengthen FBM progenitor generation. Such findings are important for the efficient in vitro generation of specific subtypes of motorneuron progenitors.

ES-Derived FBM-Like Progenitors Survive and Differentiate into Postmitotic Neurons Following Orthotopic Transplantation

These findings suggested a strong resemblance of Hoxb1⁺/SAG treated mES-derived neural progenitors to FBM neuron progenitors and they also suggested that such neural progenitors might be able to survive and differentiate following orthotopic transplantation in the mature brain. The culture conditions used here do not allow for maturation as assessed by the lack of NeuN and choline acetyl transferase (ChAT) expression in immunofluorescence experiments. To assess whether these cells were able to survive and mature in vivo, we genetically labeled the ES$^{\text{Tet-On/Hoxb1}}$ mES line by incorporating in the ROSA26 locus, through homologous recombination, an EFGP transgene driven by the constitutively strong CAG promoter[54] (Supplementary Fig. S5A). The resulting ES$^{\text{Tet-On/Hoxb1/GFP}}$ cells were differentiated into FBM-like progenitors as shown in Fig. 4A. Cells that underwent the same procedure with the exception of dox treatment gave rise to neural cells that were used as controls. Approximately 5000 FBM-like progenitors or control neural cells suspended in 1 μL were grafted stereotactically close to the facial nucleus of adult wild-type mice (Fig. 5A) as well as in the cerebellum as a control ectopic transplantation site. Following the transplantation procedure, the mice did not show any unusual behavior and the first mice were sacrificed after 1 month. Cells in the orthotopic grafts of FBM-like progenitors survived (n = 2), whereas a graft of control cells close to the facial nucleus (n = 1) did not survive. Cells in the FBM-like progenitor grafts were NeuN⁺ but did not express ChAT and we decided to extend the period after transplantation and animals were sacrificed after 6 months. Grafts of FBM-like progenitor cells near the facial nucleus survived well (14/15) while none of the cerebellum grafts (0/6) was detectable after 6 months. Grafts of control cells also showed low survival irrespective of whether the transplantation site was the facial nucleus or the cerebellum (2/8 and 2/5, respectively), suggesting that locally provided survival signals might be necessary for the survival of these cells. We then examined whether orthotopically transplanted cells mature into acetylcholine producing motoneurons by immunofluorescence with antibodies against NeuN and ChAT. We found that stained grafts (6/7) contained numerous postmitotic NeuN⁺ neurons and occasionally (3/7) some ChAT⁺ neurons (Fig. 5B, D and C, E in high magnification).

These findings suggested that a combination of directed neural differentiation, inducible *Hoxb1* expression and shh signaling stimulation resulted into FBM—like cells that can survive and mature into postmitotic neurons following orthotopic transplantation close to the facial nucleus. Refinement of this approach and extension into MN progenitors specified through the action of more posterior *Hox* genes could result in an array of MN progenitors corresponding to different axial levels that could survive and mature in vivo with implications for neurodegenerative diseases.

Discussion

The molecular functions of *Hox* genes have intrigued developmental biologists for decades. Their recurrent employment in derivatives of all 3 germ layers and at different time points compounds the complexity of unraveling their functions. The search for Hox downstream genes has identified diverse factors with broad regulatory developmental functions as well as the so-called "realisator" genes that are more directly involved in morphogenetic processes.[2,55,56] Whereas it is accepted that the context dependent activity of *Hox* genes lies at the roots of the diversity of downstream effectors, the interplay of *Hox* genes with extracellular signals in shaping developmental processes has not been adequately examined. Here, taking advantage of appropriate mES cell in vitro differentiation protocols,[18,35] we have addressed this issue by examining the interaction of Hoxb1 with signaling

pathways in 2 different cellular contexts, NMPs and neural progenitors.

The discovery of the bipotent NMPs that contribute to both the spinal cord and paraxial mesoderm in the mouse embryo[13] and subsequent studies that derived such cells in vitro from human or mouse PS cells[18,57] led to the revision of the classical Niewkoop neural activation/ transformation model.[58] These findings established that posterior neural tissue is generated independently of the mechanism(s) involved in the induction of the anterior neural plate. Neuromesodermal progenitors are localized in the caudal lateral epiblast and adjacent to the node-streak border,[14,15] arise early in development and persist as a population during axis elongation fueling the posterior growth of the body axis. *Hox* genes are sequentially activated in NMPs and this was recapitulated in vitro when NMPs were maintained in culture for several days.[18,59] Sequential *Hox* gene activation is constrained by intrinsic chromatin based timing mechanisms but these are dependent upon temporal changes of extrinsic cues.[60] A study of the *Hox* clock pacing in human PS cell derived NMPs showed that the activation of the caudal *Hox* genes is controlled by a dynamic increase in FGF signaling.[61] Are *Hox* genes passive bystanders or participants in this process? The NMPs generated here correspond to an early state as suggested by the strong expression of *Hoxb1* and *Hoxb2*, reasonable levels of expression of Hox3 members but weak or absent expression of other *Hox* genes (Supplementary Table S2). *Hoxb1* inactivation led to a dramatic downregulation of *Hoxb2* as well as downregulation of all other expressed *Hox* genes (Supplementary Table S2) but NMP identity was not affected (Supplementary Fig. S1D), suggesting that *Hox* gene function is not a prerequisite for the establishment of NMPS. Direct auto- and cross-activation of *Hox* genes has been amply demonstrated,[62-66] but it remains to be seen to what extent posterior cues such as FGFs and GDF11 are direct targets of Hox transcription factors. Our results suggested that anterior *Hox* genes, *Hoxb1* in particular, activate *Fgf8* and *Fgf17* expression as well as components of the Fgf signaling pathway and that this activation is necessary for NMP survival, a function that has also been attributed to Hoxb1 in the context of FBMs.[29-31] Thus, we propose that *Hox* genes activate Fgf signaling as well as more posterior *Hox* genes. This leads to increased activation of FGF signaling that induces the expression of additional, more posterior *Hox* genes through activation of *Cdx* genes that clear repressive chromatin marks.[67,68] This establishes an autocrine, self—sustaining, feed forward loop until the activation of posterior *Hox* genes and eventually the paralogous group 13 *Hox* genes increasingly repress Wnt signaling, effectively terminating cell proliferation.[57,69] Hoxb1 expression was necessary in vitro for NMP survival but it is apparently not necessary in vivo (Supplementary Fig. S1A) as also demonstrated by the absence of elongation defects in the *Hoxb1* null embryos.[30,31] This difference is most likely due to the expression of several other *Hox* genes in vivo at the time (9.5 dpc) of analysis and illustrates the reductionist power of this model system.

Exposure of NMPs at different time points to RA induced neural differentiation and resulted in motorneurons with anterior-posterior identities according to the combination of Hox genes expressed at the time of RA addition.[59] These findings supported the proposed model whereby exposure to FGF8/Wnt signaling progressively activates more posterior Hox genes, whereas exposure to RA inhibits so arrests the temporal progression of 3′-5′ Hox gene expression, thereby setting the Hox code as differentiation is initiated.[19] The patterning of the neural tube proceeds under the influence of dorsal and ventral morphogens[70] and the role of *Hox* genes in assigning neuronal identity has been well established, in line with their conserved roles in body patterning and particularly with regards to motorneurons.[71] Manipulation of *Hox* gene expression in mouse and chick embryos can modify both motorneuron subtype specification and axonal projection patterns establishing that Hox genes play a central role in these processes. However, the interaction of Hox genes themselves with neural tube patterning signals has not yet been fully explored. Here we show that, surprisingly, Hoxb1 synergizes with shh signaling in mES cell-derived neural progenitors in suppressing anterior identity and refining hindbrain identity. Additionally, it synergizes with shh in suppressing dorsal fates while inducing ventral identities. This interaction extends to the induction of additional signals and signal receptors that may help further refine the molecular identity of neuronal subtypes and promote their differentiation. A case in point is the expression of the receptor tyrosine kinase Ret that promotes trunk MN survival.[52] Hoxb1 and shh synergistically activate Ret expression in mES cell-derived neural progenitors and addition of the Ret ligand GDNF strongly enhances upregulation of Isl1 and Phox2b, which are key determinants of the FBM identity.[51] Thus, the synergistic interaction of Hoxb1 and shh induce Ret which mediates further differentiation into FBM identity suggesting another Hox mediated feed forward loop in a different cellular context. Regulation of the TNF/NF-kB and Notch signaling pathways by *Hox* genes in diverse contexts[10,20,35,72,73] raises the possibility that this is a widespread yet underappreciated aspect of Hox gene function.

The ability of Hox transcription factors to play central roles in the refinement of cell identity appears surprising given the high degree of conservation of the homeobox DNA-binding domain. At a first level, specificity is provided by various DNA binding ubiquitous factors such as the general Pbx and Meis proteins[3,74] or other context-specific transcription factors such as Foxp1[75] and at a second level by subtle changes in the binding specificities and differential ability to engage inaccessible chromatin across Hox paralogous groups.[76-78] Hox proteins can function as both activators and repressors[79-81] and in view of the results described here we speculate that synergistic binding of Hox proteins with diverse signaling pathway effectors may serve as a means of increasing binding specificity as well as fulfilling the context dependent functions of Hox genes. ChIP Seq assays at different cellular contexts will be necessary to elucidate this issue. Research into the molecular underpinnings of MN specification during development has enabled their in vitro application for the generation of large numbers of such cells for further mechanistic studies[71] but precise axial specification, purity, and maturation remain issues to be addressed. The in vitro generation of NMPs and the recapitulation of the Hox clock in vitro[18,59] have opened new possibilities to generate posterior neural cells with precise AP identity. Understanding the interactions of *Hox* genes with signaling pathways in different stages of development will promote the identification of signals which can be employed to establish and maintain specific neuronal cell types. Our transplantation experiments suggested that appropriate manipulation

of Hox axial identity and signaling pathways can generate cells that will survive longer and mature when transplanted orthotopically. A multi-step approach combining the establishment of proper axial identity in hPS cell-derived NMPS and the subsequent timely application of appropriate signals could be the blueprint to generate motorneurons and neurons that will survive and functionally integrate following transplantation, with implications for disease modelling, mechanistic studies and possibly therapies.

Acknowledgments

We thank Mina Gouti for advice regarding the derivation of the ES lines and NMP derivation as well as for critically reading the manuscript and providing comments and the personnel of the animal house at CRTD for help with animal husbandry. Research in AG's laboratory was supported by grants from the German Center for Diabetes Research (DZD) (grant 82DZD00101), the German Research Foundation (DFG) (SFB 655, CRTD Seed Grant 2014) as well as a TU Dresden Graduate Academy Bridging Grant to K.P.

Conflict of Interest

The authors declared no potential conflicts of interest.

Author Contributions

K.P.: performed laboratory work, data analysis and interpretation, manuscript editing, final approval of manuscript, I.G.: performed laboratory work, final approval of manuscript, M.L.: performed RNA Sequencing analysis and interpretation, final approval of the manuscript, E.R.-A.: performed laboratory work, manuscript editing, final approval of manuscript, A.G.: conception/design and fundraising, data analysis and interpretation, manuscript writing, final approval of the manuscript.

Data Availability

No new data were generated or analyzed in support of this research.

References

1. Krumlauf R. *Hox* genes in vertebrate development. *Cell*. 1994;78:191-201. https://doi.org/10.1016/0092-8674(94)90290-9
2. Rezsohazy R, Saurin AJ, Maurel-Zaffran C, et al. Cellular and molecular insights into Hox protein action. *Development*. 2015;142(7):1212-1227. https://doi.org/10.1242/dev.109785
3. Moens CB, Selleri L. Hox cofactors in vertebrate development. *Dev Biol*. 2006;291(2):193-206. https://doi.org/10.1016/j.ydbio.2005.10.032
4. Donaldson IJ, Amin S, Hensman JJ, et al. Genome-wide occupancy links Hoxa2 to Wnt-beta-catenin signaling in mouse embryonic development. *Nucleic Acids Res*. 2012;40(9):3990-4001. https://doi.org/10.1093/nar/gkr1240
5. Jung H, Lacombe J, Mazzoni EO, et al. Global control of motor neuron topography mediated by the repressive actions of a single hox gene. *Neuron*. 2010;67(5):781-796. https://doi.org/10.1016/j.neuron.2010.08.008
6. Lee HM, Zhang H, Schulz V, et al. Downstream targets of HOXB4 in a cell line model of primitive hematopoietic progenitor cells. *Blood*. 2010;116(5):720-730. https://doi.org/10.1182/blood-2009-11-253872
7. Rinn JL, Wang JK, Allen N, et al. A dermal HOX transcriptional program regulates site-specific epidermal fate. *Genes Dev*. 2008;22(3):303-307. https://doi.org/10.1101/gad.1610508
8. Oshima M, Endoh M, Endo TA, et al. Genome-wide analysis of target genes regulated by HoxB4 in hematopoietic stem and progenitor cells developing from embryonic stem cells. *Blood*. 2011;117(15):e142-e150. https://doi.org/10.1182/blood-2010-12-323212
9. Takemoto T, Uchikawa M, Kamachi Y, et al. Convergence of Wnt and FGF signals in the genesis of posterior neural plate through activation of the Sox2 enhancer N-1. *Development*. 2006;133(2):297-306. https://doi.org/10.1242/dev.02196
10. De Kumar B, Parker HJ, Parrish ME, et al. Dynamic regulation of Nanog and stem cell-signaling pathways by Hoxa1 during early neuro-ectodermal differentiation of ES cells. *Proc Natl Acad Sci USA*. 2017;114(23):5838-5845. https://doi.org/10.1073/pnas.1610612114
11. Niehrs C. Regionally specific induction by the Spemann-Mangold organizer. *Nat Rev Genet*. 2004;5(6):425-434. https://doi.org/10.1038/nrg1347
12. Andoniadou CL, Martinez-Barbera JP. Developmental mechanisms directing early anterior forebrain specification in vertebrates. *Cell Mol Life Sci*. 2013;70(20):3739-3752. https://doi.org/10.1007/s00018-013-1269-5
13. Tzouanacou E, Wegener A, Wymeersch FJ, et al. Redefining the progression of lineage segregations during mammalian embryogenesis by clonal analysis. *Dev Cell*. 2009;17(3):365-376. https://doi.org/10.1016/j.devcel.2009.08.002
14. Cambray N, Wilson V. Two distinct sources for a population of maturing axial progenitors. *Development*. 2007;134(15):2829-2840. https://doi.org/10.1242/dev.02877
15. Olivera-Martinez I, Storey KG. Wnt signals provide a timing mechanism for the FGF-retinoid differentiation switch during vertebrate body axis extension. *Development*. 2007;134(11):2125-2135. https://doi.org/10.1242/dev.000216
16. Henrique D, Abranches E, Verrier L, et al. Neuromesodermal progenitors and the making of the spinal cord. *Development*. 2015;142(17):2864-2875. https://doi.org/10.1242/dev.119768
17. Martin BL, Kimelman D. Regulation of canonical Wnt signaling by Brachyury is essential for posterior mesoderm formation. *Dev Cell*. 2008;15(1):121-133. https://doi.org/10.1016/j.devcel.2008.04.013
18. Gouti M, Tsakiridis A, Wymeersch FJ, et al. In vitro generation of neuromesodermal progenitors reveals distinct roles for wnt signalling in the specification of spinal cord and paraxial mesoderm identity. *PLoS Biol*. 2014;12(8):e1001937. https://doi.org/10.1371/journal.pbio.1001937
19. Diez del Corral R, Storey KG. Opposing FGF and retinoid pathways: a signalling switch that controls differentiation and patterning onset in the extending vertebrate body axis. *Bioessays*. 2004;26(8):857-869. https://doi.org/10.1002/bies.20080
20. Gouti M, Briscoe J, Gavalas A. Anterior Hox genes interact with components of the neural crest specification network to induce neural crest fates. *Stem Cells*. 2011;29(5):858-870. https://doi.org/10.1002/stem.630
21. Alexander T, Nolte C, Krumlauf R. Hox genes and segmentation of the hindbrain and axial skeleton. *Annu Rev Cell Dev Biol*. 2009;25:431-456. https://doi.org/10.1146/annurev.cellbio.042308.113423
22. Parker HJ, Bronner ME, Krumlauf R. The vertebrate Hox gene regulatory network for hindbrain segmentation: evolution and diversification: coupling of a Hox gene regulatory network to hindbrain segmentation is an ancient trait originating at the base of vertebrates. *Bioessays*. 2016;38(6):526-538. https://doi.org/10.1002/bies.201600010
23. Chisaka O, Musci T, Capecchi M. Developmental defects of the ear, cranial nerves and hindbrain resulting from targeted disruption of the mouse homeobox gene *Hox-1.6*. *Nature*. 1992;355:516-520.
24. Gavalas A, Trainor P, Ariza-McNaughton L, et al. Synergy between Hoxa1 and Hoxb1: the relationship between arch patterning

and the generation of cranial neural crest. *Development*. 2001;128(15):3017-3027.
25. Lufkin T, Dierich A, LeMeur M, et al. Disruption of the *Hox-1.6* homeobox gene results in defects in a region corresponding to its rostral domain of expression. *Cell*. 1991;66(6):1105-1119. https://doi.org/10.1016/0092-8674(91)90034-v
26. Gavalas A, Studer M, Lumsden A, et al. *Hoxa1* and *Hoxb1* synergize in patterning the hindbrain, cranial nerves and second pharyngeal arch. *Development*. 1998;125:1123-1136.
27. Gavalas A, Trainor P, Ariza-McNaughton L, et al. Synergy between Hoxa1 and Hoxb1: the relationship between arch patterning and the generation of cranial neural crest*Development*. 2001;128(15):3017-3027. [in English].
28. Samad OA, Geisen MJ, Caronia G, et al. Integration of anteroposterior and dorsoventral regulation of Phox2b transcription in cranial motoneuron progenitors by homeodomain proteins. *Development*. 2004;131(16):4071-4083. https://doi.org/10.1242/dev.01282
29. Gavalas A, Ruhrberg C, Livet J, et al. Neuronal defects in the hindbrain of Hoxa1, Hoxb1 and Hoxb2 mutants reflect regulatory interactions among these Hox genes. *Development*. 2003;130(23):5663-5679. [in English]. https://doi.org/10.1242/dev.00802
30. Goddard J, Rossel M, Manley N, et al. Mice with targeted disruption of *Hoxb1* fail to form the motor nucleus of the VIIth nerve. *Development*. 1996;122:3217-3228.
31. Studer M, Lumsden A, Ariza-McNaughton L, et al. Altered segmental identity and abnormal migration of motor neurons in mice lacking *Hoxb-1*. *Nature*. 1996;384:630-634. https://doi.org/10.1038/384630a0
32. Bonito M D, Narita Y, Avallone B, et al. Assembly of the auditory circuitry by a Hox genetic network in the mouse brainstem. *PLoS Genet*. 2013;9(2):e1003249.
33. Webb BD, Shaaban S, Gaspar H, et al. HOXB1 founder mutation in humans recapitulates the phenotype of Hoxb1-/- mice. *Am J Hum Genet*. 2012;91(1):171-179. https://doi.org/10.1016/j.ajhg.2012.05.018
34. Vogel M, Velleuer E, Schmidt-Jimenez LF, et al. Homozygous HOXB1 loss-of-function mutation in a large family with hereditary congenital facial paresis. *Am J Med Genet A*. 2016;170(7):1813-1819. https://doi.org/10.1002/ajmg.a.37682
35. Gouti M, Gavalas A. Hoxb1 controls cell fate specification and proliferative capacity of neural stem and progenitor cells. *Stem Cells*. 2008;26(8):1985-1997. https://doi.org/10.1634/stemcells.2008-0182
36. Wu TD, Nacu S. Fast and SNP-tolerant detection of complex variants and splicing in short reads [in eng]. *Bioinformatics*. 2010;26(7):873-881. https://doi.org/10.1093/bioinformatics/btq057
37. Wu TD, Watanabe CK. GMAP: a genomic mapping and alignment program for mRNA and EST sequences. *Bioinformatics*. 2005;21(9):1859-1875. https://doi.org/10.1093/bioinformatics/bti310
38. Liao Y, Smyth GK, W S. featureCounts: an efficient general purpose program for assigning sequence reads to genomic features [Research Support, Non-U.S. Gov't. *Bioinformatics*. 2014;30(7):923-930. [in English].
39. Love MI, Huber W, Anders S. Moderated estimation of fold change and dispersion for RNA-seq data with DESeq2 [Research Support, N.I.H., Extramural Research Support, Non-U.S. Gov't. *Genome Biol*. 2014;15(12):550. [in English]. https://doi.org/10.1186/s13059-014-0550-8
40. Gavalas A, Pazur K. The role of Hoxb1 in NMPs and neural progenitors [Data repository]. *GEO* 2021:GSE174021.
41. Huang da W, Sherman BT, Lempicki RA. Systematic and integrative analysis of large gene lists using DAVID bioinformatics resources. *Nat Protoc*. 2009;4(1):44-57.
42. Huang da W, Sherman BT, Lempicki RA. Bioinformatics enrichment tools: paths toward the comprehensive functional analysis of large gene lists. *Nucleic Acids Res*. 2009;37(1):1-13.
43. Studer M, Gavalas A, Marshall H, et al. Genetic interactions between Hoxa1 and Hoxb1 reveal new roles in regulation of early hindbrain patterning. *Development*. 1998;125(6):1025-1036.
44. Ying QL, Wray J, Nichols J, et al. The ground state of embryonic stem cell self-renewal. *Nature*. 2008;453(7194):519-523. https://doi.org/10.1038/nature06968
45. Wilson V, Olivera-Martinez I, Storey KG. Stem cells, signals and vertebrate body axis extension. *Development*. 2009;136(10):1591-1604. https://doi.org/10.1242/dev.021246
46. Maruoka Y, Ohbayashi N, Hoshikawa M, et al. Comparison of the expression of three highly related genes, Fgf8, Fgf17 and Fgf18, in the mouse embryo. *Mech Dev*. 1998;74(1-2):175-177. https://doi.org/10.1016/s0925-4773(98)00061-6
47. Gouti M, Delile J, Stamataki D, et al. A Gene regulatory network balances neural and mesoderm specification during vertebrate trunk development. *Dev Cell*. 2017;41(3):243-261.e7. https://doi.org/10.1016/j.devcel.2017.04.002
48. Chen JK, Taipale J, Young KE, et al. Small molecule modulation of Smoothened activity. *Proc Natl Acad Sci USA*. 2002;99(22):14071-14076. https://doi.org/10.1073/pnas.182542899
49. Prakash N, Puelles E, Freude K, et al. Nkx6-1 controls the identity and fate of red nucleus and oculomotor neurons in the mouse midbrain. *Development*. 2009;136(15):2545-2555. https://doi.org/10.1242/dev.031781
50. Shimamura K, Hartigan DJ, Martinez S, et al. Longitudinal organization of the anterior neural plate and neural tube. *Development*. 1995;121(12):3923-3933.
51. Song MR, Shirasaki R, Cai CL, et al. T-Box transcription factor Tbx20 regulates a genetic program for cranial motor neuron cell body migration. *Development*. 2006;133(24):4945-4955. https://doi.org/10.1242/dev.02694
52. Catela C, Shin MM, Lee DH, et al. Hox proteins coordinate motor neuron differentiation and connectivity programs through Ret/Gfralpha genes. *Cell Rep*. 2016;14(8):1901-1915. https://doi.org/10.1016/j.celrep.2016.01.067
53. Baudet C, Pozas E, Adameyko I, et al. Retrograde signaling onto Ret during motor nerve terminal maturation. *J Neurosci*. 2008;28(4):963-975. https://doi.org/10.1523/JNEUROSCI.4489-07.2008
54. Niwa H, Yamamura K, Miyazaki J. Efficient selection for high-expression transfectants with a novel eukaryotic vector. *Gene*. 1991;108(2):193-199. https://doi.org/10.1016/0378-1119(91)90434-d
55. Parker HJ, Pushel I, Krumlauf R. Coupling the roles of Hox genes to regulatory networks patterning cranial neural crest. *Dev Biol*. 2018;444(Suppl 1):S67-S78. https://doi.org/10.1016/j.ydbio.2018.03.016
56. Hueber SD, Bezdan D, Henz SR, et al. Comparative analysis of Hox downstream genes in Drosophila. *Development*. 2007;134(2):381-392. https://doi.org/10.1242/dev.02746
57. Turner DA, Hayward PC, Baillie-Johnson P, et al. Wnt/beta-catenin and FGF signalling direct the specification and maintenance of a neuromesodermal axial progenitor in ensembles of mouse embryonic stem cells. *Development*. 2014;141(22):4243-4253. https://doi.org/10.1242/dev.112979
58. Nieuwkoop P. Activation and organisation of the central nervous system in amphibians. *J Exp Zool*. 1952;120:1-108.
59. Lippmann ES, Williams CE, Ruhl DA, et al. Deterministic HOX patterning in human pluripotent stem cell-derived neuroectoderm. *Stem Cell Rep*. 2015;4(4):632-644. https://doi.org/10.1016/j.stemcr.2015.02.018
60. Deschamps J, Duboule D. Embryonic timing, axial stem cells, chromatin dynamics, and the Hox clock. *Genes Dev*. 2017;31(14):1406-1416. https://doi.org/10.1101/gad.303123.117
61. Mouilleau V, Vaslin C, Robert R, et al. Dynamic extrinsic pacing of the HOX clock in human axial progenitors controls motor neuron subtype specification. *Development*. 2021;148(6). https://doi.org/10.1242/dev.194514
62. Gould A, Morrison A, Sproat G, et al. Positive cross-regulation and enhancer sharing: two mechanisms for specifying overlapping *Hox*

expression patterns. *Genes Dev.* 1997;11:900-913. https://doi.org/10.1101/gad.11.7.900
63. Maconochie M, Nonchev S, Studer M, et al. Cross-regulation in the mouse *HoxB* complex: the expression of *Hoxb2* in rhombomere 4 is regulated by *Hoxb1 Genes Dev.* 1997;11:1885-1896.
64. Manzanares M, Bel-Vialar S, Ariza-McNaughton L et al. Independent regulation of initiation and maintenance phases of Hoxa3 expression in the vertebrate hindbrain involve auto- and cross- regulatory mechanisms. *Development* 2001;128(18):3595-3607.
65. Packer A, Crotty D, Elwell V, et al. Expression of the murine Hoxa4 gene requires both autoregulation and a conserved retinoic acid response element. *Development*. 1998;125:1991-1998. https://doi.org/10.1242/dev.125.11.1991
66. Pöpperl H, Bienz M, Studer M, et al. Segmental expression of *Hoxb1* is controlled by a highly conserved autoregulatory loop dependent upon *exd/Pbx*. *Cell.* 1995;81:1031-1042. https://doi.org/10.1016/s0092-8674(05)80008-x
67. Mazzoni EO, Mahony S, Peljto M, et al. Saltatory remodeling of Hox chromatin in response to rostrocaudal patterning signals. *Nat Neurosci*. 2013;16(9):1191-1198. https://doi.org/10.1038/nn.3490
68. Bel-Vialar S, Itasaki N, Krumlauf R. Initiating Hox gene expression: in the early chick neural tube differential sensitivity to FGF and RA signaling subdivides the HoxB genes in two distinct groups. *Development* 2002;129(22):5103-5115.
69. Young T, Rowland JE, van de Ven C, et al. Cdx and Hox genes differentially regulate posterior axial growth in mammalian embryos. *Dev Cell.* 2009;17(4):516-526. https://doi.org/10.1016/j.devcel.2009.08.010
70. Sagner A, Briscoe J. Establishing neuronal diversity in the spinal cord: a time and a place. *Development*. 2019;146(22). https://doi.org/10.1242/dev.182154
71. Davis-Dusenbery BN, Williams LA, Klim JR, et al. How to make spinal motor neurons. *Development*. 2014;141(3):491-501. https://doi.org/10.1242/dev.097410
72. Taminiau A, Draime A, J T, et al. HOXA1 binds RBCK1/HOIL-1 and TRAF2 and modulates the TNF/NF-kappaB pathway in a transcription-independent manner. *Nucleic Acids Res*. 2016;44(15):7331-7349.
73. Zhang H, Xie J, So KKH, et al. Hoxb3 regulates Jag1 expression in pharyngeal epithelium and affects interaction with neural crest cells. *Front Physiol.* 2020;11:612230.
74. Bridoux L, Zarrineh P, Mallen J, et al. HOX paralogs selectively convert binding of ubiquitous transcription factors into tissue-specific patterns of enhancer activation. *PLoS Genet*. 2020;16(12):e1009162. https://doi.org/10.1371/journal.pgen.1009162
75. Philippidou P, Dasen JS. Hox genes: choreographers in neural development, architects of circuit organization. *Neuron*. 2013;80(1):12-34. https://doi.org/10.1016/j.neuron.2013.09.020
76. Bulajic M, Srivastava D, Dasen JS, et al. Differential abilities to engage inaccessible chromatin diversify vertebrate Hox binding patterns. *Development*. 2020;147(22). https://doi.org/10.1242/dev.194761
77. Berger MF, Badis G, Gehrke AR, et al. Variation in homeodomain DNA binding revealed by high-resolution analysis of sequence preferences. *Cell*. 2008;133(7):1266-1276. https://doi.org/10.1016/j.cell.2008.05.024
78. Noyes MB, Christensen RG, Wakabayashi A, et al. Analysis of homeodomain specificities allows the family-wide prediction of preferred recognition sites. *Cell*. 2008;133(7):1277-1289. https://doi.org/10.1016/j.cell.2008.05.023
79. Carnesecchi J, Pinto PB, Lohmann I. Hox transcription factors: an overview of multi-step regulators of gene expression. *Int J Dev Biol*. 2018;62(11-12):723-732. https://doi.org/10.1387/ijdb.180294il
80. Singh NP, De Kumar B, Paulson A, et al. Genome-wide binding analyses of HOXB1 revealed a novel DNA binding motif associated with gene repression. *J Dev Biol*. 2021;9(1). https://doi.org/10.3390/jdb9010006
81. Stefanovic S, Laforest B, Desvignes JP, et al. Hox-dependent coordination of mouse cardiac progenitor cell patterning and differentiation. *Elife*. 2020;9. https://doi.org/10.7554/eLife.55124